Measuring frequency noise and intrinsic linewidth of a room-temperature DFB quantum cascade laser

S. Bartalini,[1,2,*] S. Borri,[1,2] I. Galli,[1,2] G. Giusfredi,[1,2] D. Mazzotti,[1,2] T. Edamura,[3] N. Akikusa,[3] M. Yamanishi,[3] and P. De Natale[1,2]

[1]*Istituto Nazionale di Ottica (INO) - CNR, Largo Fermi 6, 50125 Firenze FI, Italy*
[2]*European Laboratory for Nonlinear Spectroscopy (LENS), Via Carrara 1, 50019 Sesto Fiorentino FI, Italy*
[3]*Central Research Laboratories, Hamamatsu Photonics KK, Shizuoka 434-8601, Japan*
saverio.bartalini@ino.it

Abstract: The frequency-noise power spectral density of a room-temperature distributed-feedback quantum cascade laser emitting at $\lambda = 4.36\ \mu$m has been measured. An intrinsic linewidth value of 260 Hz is retrieved, in reasonable agreement with theoretical calculations. A noise reduction of about a factor 200 in most of the frequency interval is also found, with respect to a cryogenic laser at the same wavelength. A quantitative treatment shows that it can be explained by a temperature-dependent mechanism governing the transport processes in resonant tunnelling devices. This confirms the predominant effect of the heterostructure in determining shape and magnitude of the frequency noise spectrum in QCLs.

OCIS codes: (140.5965) Semiconductor lasers, quantum cascade; (270.2500) Fluctuations, relaxations, and noise; (290.3700) Linewidth; (140.3425) Laser stabilization.

References and links

1. S. Bartalini, S. Borri, P. Cancio, A. Castrillo, I. Galli, G. Giusfredi, D. Mazzotti, L. Gianfrani, and P. De Natale, "Observing the intrinsic linewidth of a quantum-cascade laser: beyond the Schawlow–Townes limit," Phys. Rev. Lett. **104**, 083904 (2010).
2. J. Faist, F. Capasso, D. L. Sivco, C. Sirtori, A. L. Hutchinson, and A. Y. Cho, "Quantum cascade laser," Science **264**, 553–556 (1994).
3. C. Henry, "Theory of the linewidth of semiconductor lasers," IEEE J. Quantum Electron. **18**, 259–264 (1982).
4. M. Yamanishi, T. Edamura, K. Fujita, N. Akikusa, and H. Kan, "Theory of the intrinsic linewidth of quantum-cascade lasers: hidden reason for the narrow linewidth and line-broadening by thermal photons," IEEE J. Quantum Electron. **44**, 12–29 (2008).
5. D. S. Elliott, R. Roy, and S. J. Smith, "Extracavity laser band-shape and bandwidth modification," Phys. Rev. A **26**, 12–18 (1982).
6. S. Borri, S. Bartalini, P. Cancio, I. Galli, G. Giusfredi, D. Mazzotti, M. Yamanishi, and P. De Natale, "Frequency-noise dynamics of mid-infrared quantum cascade lasers," IEEE J. Quantum Electron. **47**, 984–988 (2011).
7. R. M. Williams, J. F. Kelly, J. S. Hartman, S. W. Sharpe, M. S. Taubman, J. L. Hall, F. Capasso, C. Gmachl, D. L. Sivco, J. N. Baillargeon, and A. Y. Cho, "Kilohertz linewidth from frequency-stabilized mid-infrared quantum cascade lasers," Opt. Lett. **24**, 1844–1846 (1999).
8. T. L. Myers, R. M. Williams, M. S. Taubman, C. Gmachl, F. Capasso, D. L. Sivco, J. N. Baillargeon, and A. Y. Cho, "Free-running frequency stability of mid-infrared quantum cascade lasers," Opt. Lett. **27**, 170–172 (2002).
9. K. Fujita, T. Edamura, N. Akikusa, A. Sugiyama, T. Ochiai, S. Furuta, A. Ito, M. Yamanishi, and H. Kan, "Quantum cascade lasers based on single phonon-continuum depopulation structures," Proc. SPIE **7230**, 723016 (2009).

#152334 - $15.00 USD Received 3 Aug 2011; revised 18 Aug 2011; accepted 19 Aug 2011; published 29 Aug 2011

10. K. Fujita, S. Furuta, A. Sugiyama, T. Ochiai, T. Edamura, N. Akikusa, M. Yamanishi, and H. Kan, "Room temperature, continuous-wave operation of quantum cascade lasers with single phonon resonance-continuum depopulation structures grown by metal organic vapor-phase epitaxy," Appl. Phys. Lett. **91**, 141121 (2007).
11. K. Fujita, S. Furuta, A. Sugiyama, T. Ochiai, T. Edamura, N. Akikusa, M. Yamanishi, and H. Kan, "High-performance $\lambda \sim 8.6$ μm quantum cascade lasers with single phonon-continuum depopulation structures," IEEE J. Quantum Electron. **46**, 683–688 (2010).
12. K. G. Libbrecht and J. L. Hall, "A low-noise high-speed diode laser current controller," Rev. Sci. Instrum. **64**, 2133–2135 (1993).
13. J. S. Yu, S. Slivken, A. Evans, L. Doris, and M. Razeghi, "High-power continuous-wave operation of a 6 μm quantum-cascade laser at room temperature," Appl. Phys. Lett. **83**, 2503–2505 (2003).
14. A. Vasanelli, A. Leuliet, C. Sirtori, A. Wade, G. Fedorov, D. Smirnov, G. Bastard, B. Vinter, M. Giovannini, and J. Faist, "Role of elastic scattering mechanisms in GaInAs/AlInAs quantum cascade lasers," Appl. Phys. Lett., **89**, 172120 (2006).
15. K. Fujita, M. Yamanishi, T. Edamura, A. Sugiyama, and S. Furuta, "Extremely high T_0-values ($\simeq$450 K) of long-wavelength ($\simeq$ 15 μm), low-threshold-current-density quantum-cascade lasers based on the indirect pump scheme," Appl. Phys. Lett. **97**, 201109 (2010).
16. D. Hofstetter, M. Beck, T. Aellen, and J. Faist, "High-temperature operation of distributed feedback quantum-cascade lasers at 5.3 μm," Appl. Phys. Lett. **78**, 396–398 (2001).
17. M. S. Vitiello, T. Gresch, A. Lops, V. Spagnolo, G. Scamarcio, N. Hoyler, M. Giovannini, and J. Faist, "Influence of InAs, AlAs δ layers on the optical, electronic, and thermal characteristics of strain-compensated GaInAs/AlInAs quantum-cascade lasers," Appl. Phys. Lett. **91**, 161111 (2007).
18. M. S. Vitiello, G. Scamarcio, V. Spagnolo, "Temperature dependence of thermal conductivity and boundary resistance in THz quantum cascade lasers," IEEE J. Select Top. Quantum Electron. **14**, 431–435 (2008).
19. M. S. Vitiello, V. Spagnolo, G. Scamarcio, A. Lops, Q. Yang, C. Manz, and J. Wagner, "Experimental investigation of the lattice and electronic temperatures in $Ga_{0.47}In_{0.53}As/Al_{0.62}Ga_{0.38}As_{1-x}Sb_x$ quantum-cascade lasers," Appl. Phys. Lett. **90**, 121109 (2007).
20. G. Giusfredi, S. Bartalini, S. Borri, P. Cancio, I. Galli, D. Mazzotti, and P. De Natale, "Saturated-absorption cavity ring-down spectroscopy," Phys. Rev. Lett. **104**, 110801 (2010).
21. S. Bartalini, S. Borri, and P. De Natale, "Doppler-free polarization spectroscopy with a quantum cascade laser at 4.3 μm," Opt. Express **17**, 7440–7449 (2009).
22. M. S. Taubman, T. L. Myers, B. D. Cannon, R. M. Williams, F. Capasso, C. Gmachl, D. L. Sivco, and A. Y. Cho "Frequency stabilization of quantum cascade lasers by use of optical cavities" Opt. Lett. **27**, 2164–2166 (2002).
23. G. Di Domenico, S. Schilt, and P. Thomann, "Simple approach to the relation between laser frequency noise and laser line shape," Appl. Opt. **49**, 4801–4807 (2010).

1. Introduction

The interest of the scientific community in frequency-noise properties of quantum-cascade lasers (QCLs) is growing in parallel with increasing demand of such sources for high-resolution spectroscopy and frequency metrology.

Cryogenically-operated QCLs have demonstrated a very low intrinsic linewidth [1], related to the white-noise component of their frequency noise spectrum. This peculiar feature, predicted since the very first demonstration of QCLs [2], relies on the very small Henry's linewidth enhancement factor and on the huge increase of the number of photons coupled to the lasing mode occurring just above threshold. This latter effect, that is already taken into account by the Schawlow-Townes formula [3], has been deeply investigated from both the theoretical and experimental point of view [4] and marks a big difference with respect to conventional bipolar lasers. However, a small intrinsic linewidth, for its own sake, does not necessarily mean that the QCL emission can be easily narrowed: when its frequency noise spectrum is also well behaved at lower frequencies, then locking loops with only moderate gains and bandwidths are needed to achieve narrow linewidths and low energy content in the wings of the emission spectrum.

As is well known, the most complete characterization of the spectral purity of a laser is the measurement of its frequency-noise power spectral density (FNPSD), since its allows the emission spectrum to be derived over any accessible timescale [5]. Besides the interest related to the implementation of ultra-narrow mid-infrared sources, the study of FNPSD in QCLs can help understanding the physics of the transport processes inside the laser heterostructure. In

#152334 - $15.00 USD Received 3 Aug 2011; revised 18 Aug 2011; accepted 19 Aug 2011; published 29 Aug 2011

particular, the operating temperature of the device was already predicted [6] to play a key role for the frequency noise of the laser, since several mechanisms contributing to noise (such as carrier transport processes in resonant tunnelling heterostructures) are expected to depend on frequency, as well as on the specific heat of the QCL. This latter quantity, in particular, is expected to affect FNPSD, as it eventually sets a thermal cut-off for the dissipative current-to-frequency-conversion mechanisms occurring in the laser, thus affecting the current-related portion of the noise spectrum. From this point of view, the comparative measurements of the FNPSD of two QCLs operating at similar wavelengths but at two different temperatures (80 K and 290 K) offers a unique opportunity for testing the hypotheses outlined above.

In the present work, following the methods described in Ref. [1], we measure the FNPSD of a room-temperature (RT) QCL working at 4.36 μm and we compare it with the same quantity already measured for a cryogenic QCL at 4.33 μm. The much lower overall FNPSD, shown by the RT device, is discussed, as well as the noise contribution from the current driver. For frequencies higher than 30 MHz a white-noise region is observed, corresponding to an intrinsic linewidth of about 260 Hz. The comparison with the expected value is discussed in depth, evidencing a good agreement with the theoretical model. The dependence on temperature of both the intrinsic linewidth and the low-frequency $1/f$–type FNPSD is also explained. In the last part of the paper we briefly discuss some perspectives concerning narrowing of QCL linewidth, showing that the reduced FNPSD enables to achieve sub-kHz linewidth with standard frequency-locking techniques.

2. Experimental setup

In the experiment, the frequency noise of the QCL is retrieved from a measurement of the intensity fluctuations of the laser beam after interaction with a frequency-to-amplitude converter. Following a well established method [7, 8], the adopted discriminator is the side of the direct-absorption profile of a molecular transition. The spectrum of the transmitted intensity, when the laser frequency ν_0 is stabilized at the half-height position, reproduces the spectrum of the laser frequency fluctuations, scaled by the slope of the absorption profile. Fig. 1 shows the concept scheme of the experimental set-up.

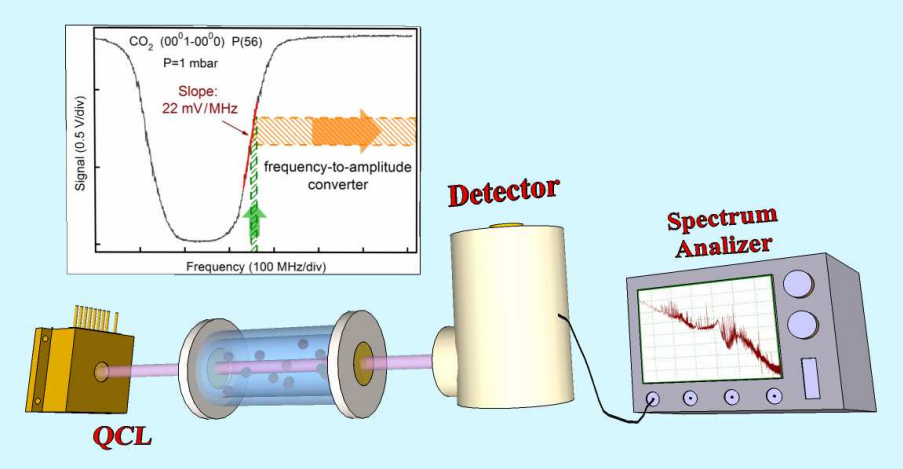

Fig. 1. The schematic shows the simple experimental setup used for the measurement of the QCL frequency-noise PSD. In the inset, an acquisition of the molecular absorption profile is also shown, and the working principle of the conversion of frequency fluctuations into amplitude fluctuations is depicted.

#152334 - $15.00 USD Received 3 Aug 2011; revised 18 Aug 2011; accepted 19 Aug 2011; published 29 Aug 2011

The molecular ro-vibrational transition used in this case is the ($00^0$1-$00^0$0) P(56) line of CO_2, at a constant pressure of 1 mbar. At this pressure, the conversion coefficient of 22 mV/MHz is maximum, providing the highest sensitivity. Considering the 30 nV/$\sqrt{\text{Hz}}$ output voltage noise of the 200-MHz-bandwidth HgCdTe photovoltaic detector used, an ultimate sensitivity of about 2 Hz^2/Hz for the FNPSD measurement is obtained. The transfer function of the discriminator is calculated for the experimental absorption profile according to the method described in [1].

The source is a distributed-feedback (DFB) QCL provided by Hamamatsu Photonics, with single-mode continuous-wave operation at temperatures in the range between 0 and 20 °C. The compact casing of the QCL also includes a thermo-electric cooler for efficient temperature stabilization. The beam, collimated by an aspherical ZnSe lens, is sent to a 10-cm-long cell for direct-absorption spectroscopy of CO_2 gas. The absorption signal is acquired by a HgCdTe detector and processed by a real-time FFT spectrum analyzer. The chosen operating QCL temperature during the measurement is $T = 15$ °C. At this temperature, the threshold current is $I_{th} = 674$ mA, while the molecular resonance is found at an operating current $I_o = 776$ mA, giving a ratio $I_o/I_{th} = 1.15$. In these conditions, the laser output power is about 20 mW.

The device used in the present work is a strain-compensated $In_{0.72}Ga_{0.28}As/In_{0.31}Al_{0.69}As$ DFB QCL [9] with 25 cascade stages, 12 μm bare ridge, 3 mm length, and an injector doping density of $\sim 2 \times 10^{11}$ cm^{-2}. The active region has a bound-to-bound quantum design, based on single phonon-continuum (SPC) depopulation [10, 11]. The layered structure was grown by metal organic vapour-phase epitaxy and the laser chip was mounted epi-side-down on a heat sink.

3. Measurements

We measured the FNPSD of the RT QCL with two different current drivers: in Fig. 2a the QCL is powered by the same home-made current driver used in our previous work [1], which is based on the well-known Hall–Libbrecht design [12], while in Fig. 2b a commercial current driver

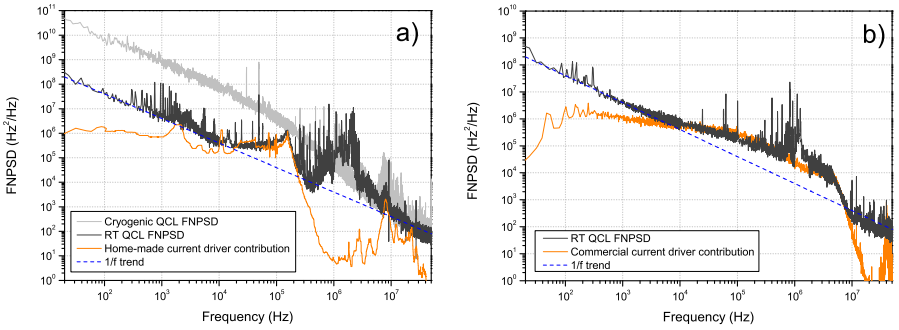

Fig. 2. a) Comparison between the FNPSDs of a cryogenic QCL (light gray, QCL_2, operating current $I_{o2} = 219$ mA) and the RT QCL studied in this work (dark gray, QCL_1, operating current $I_{o1} = 776$ mA). The level of the flicker noise is about 200 times lower for the RT device. The plot also shows how the contribution from the current noise of our home-made driver, that was negligible for the cryogenic QCL, now becomes relevant. b) The same measurement is repeated with the commercial current driver. Despite the larger noise contribution below 10 MHz, the strong filtering at higher frequencies allows a clear observation of the white intrinsic noise. The dashed blue line, showing the $1/f$ trend, is the same for both graphs.

#152334 - $15.00 USD Received 3 Aug 2011; revised 18 Aug 2011; accepted 19 Aug 2011; published 29 Aug 2011

(Wavelength Electronics, model QCL1000) is used. Both plots also report the noise contribution from the corresponding current driver. Fig. 2a shows, in addition, the FNPSD measured in our previous work for the cryogenic DFB QCL. The first remarkable result is that the FNPSD of the RT QCL is considerably below that of the cryogenic QCL in most of the investigated spectral range. For frequencies lower than 10 kHz, where both trends follow a $1/f$ behavior, the ratio between the two noise spectra is constant at about 200. In the 10-200 kHz range, the noise contribution from the current driver is dominant and hinders precise measurement of the QCL frequency noise. This was not observed with the cryogenic QCL, due to its larger FNPSD. Between 1 MHz and 10 MHz the RT QCL shows a noise feature not originating from the current noise and resulting from an envelope of adjacent spikes. We think that this technical noise could arise from a non-optimized electrical grounding of the RT QCL. Finally, above 10 MHz, both the current noise of the home-made driver and the technical noise are negligible, allowing the pure QCL frequency noise to emerge. Despite the spurious contributions described above, we can state that all the FNPSD of the QCL (before the white-noise flattening) is consistent with an $1/f$ behavior.

The situation is slightly different when the commercial current driver is used (see Fig. 2b). Here, the larger contribution from the current noise is even more dominant below 10 MHz, and prevents any useful interpretation. However, above 10 MHz, the commercial driver current noise drastically drops down, allowing a clean measurement of the QCL FNPSD, in agreement with what is measured with the home-made driver. A zoom of this last portion of both spectra is shown in Fig.3: the flattening of the FNPSD down to a white-noise level (N_w) is evident, and yields an intrinsic linewidth $\delta\nu_{exp} = \pi N_w = 260 \pm 90$ Hz, about four times smaller than that measured for the cryogenic QCL at the same value of I_o/I_{th} (1.15). The uncertainty is calculated by taking into account both the scattering of the data in a single trace and the slope calibration error.

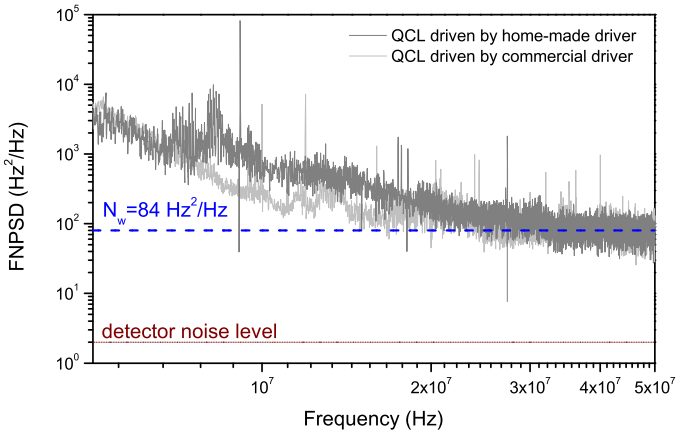

Fig. 3. The plot shows in detail the high-frequency portion of the measured FNPSD, where a flattening down to a white-noise level of 84 Hz^2/Hz occurs. The sensitivity of our system is also represented by the detector noise level.

4. Discussion

The experimental value of the intrinsic linewidth can be compared with theory by evaluating the Schawlow-Townes-Henry formula. Alternatively, we prefer to use the approach adopted in our previous work [1], inspired by the theoretical treatment of Ref. [4]. The intrinsic linewidth,

#152334 - $15.00 USD Received 3 Aug 2011; revised 18 Aug 2011; accepted 19 Aug 2011; published 29 Aug 2011

referring to a 3-level model, can be written as:

$$\delta\nu = \frac{1}{4\pi}\frac{\gamma\beta_{eff}}{(1-\varepsilon)}\cdot\left[\frac{1}{(I_o/I_{th}-1)}+\varepsilon\right]\cdot(1+\alpha_e^2), \tag{1}$$

with

$$\beta_{eff} = \beta\frac{\tau_t}{\tau_r}, \quad \varepsilon = \frac{\tau_{21}\tau_{31}}{\eta\tau_t(\tau_{21}+\tau_{31})} \simeq \frac{\tau_{21}}{\eta\tau_t}, \quad \alpha_e \simeq 0. \tag{2}$$

The parameters involved in the formula above are provided and discussed below, and we refer to Ref. [4] and equations therein (in particular Equations A6, A11 and A14) for their numerical estimation. For the sake of brevity, we will also refer to the RT QCL measured in the present work as QCL_1, and to the cryogenic QCL used in our previous work [1] as QCL_2. Due to the CW-operation, all the parameters must be calculated at active region temperatures. At threshold, $I_{th} = 674$ mA for QCL_1, the active region temperature is determined to be the temperature giving, in pulsed operation, the same threshold current as in CW-operation, namely $\sim$ 340 K, about 50 K higher than the heat-sink temperature $T \sim$290 K (see Ref. [13]). For QCL_1, it results an active region temperature $T_1 \sim$350 K at the bias conditions $I_0 = 776$ mA and $V_{bias} = 10$ V (with a thermal resistance $R_{therm1} \sim 7.42$ K/W). With a different manner, the active region temperature of QCL_2 (at its experimental bias conditions $I_0 = 219$ mA and $V_{bias} = 10$ V) is $T_2 \sim 182$ K, about 97 K higher than the heat-sink temperature $T = 85$ K (see discussion for the higher thermal resistance $R_{therm2} \sim 44.5$ K/W of QCL_2, below Eq. 3).

Focusing on QCL_1 at the active region temperature T_1, the non-radiative relaxation times due to LO-phonons and temperature-insensitive elastic (alloy-disorder) scattering processes [14,15] are $\tau_t \approx \tau_3 \sim 1$ ps, $\tau_{31} \sim 1.7$ ps and $\tau_{21} \sim 0.15$ ps, while the radiative lifetime of the upper laser level, due to spontaneous emission, $\tau_r \sim 10$ ns, is four orders of magnitude longer than τ_t. Similarly, the key parameter $\beta_{eff} = \beta\tau_t/\tau_r \sim 5\times10^{-9}$, called "effective coupling efficiency", is four orders of magnitude smaller than the spontaneous emission coupling efficiency, $\beta \sim 5\times10^{-5}$. With an injection efficiency $\eta \sim 0.7$, a photon decay rate $\gamma \sim 1\times10^{11}$ s^{-1} and $\alpha_e \sim 0$, an intrinsic linewidth $\delta\nu \sim 340$ Hz at $I_0/I_{th} = 1.15$ and a threshold current $I_{th} \sim 430$ mA are obtained, the latter estimated by equations (11) and (12) in Ref. [4], assuming an energy separation $E_{21} \sim 130$ meV (value from design [9]). By slightly adjusting the parameters related to optical processes $\gamma \sim 1.2\times10^{11}$ s^{-1}, and $\beta_{eff} \sim 3\times10^{-9}$, while leaving unchanged the relaxation times and the injection efficiency η, we obtain $\delta\nu \sim 245$ Hz at $I_0/I_{th} = 1.15$ and $I_{th} \sim 634$ mA. The excellent agreement with the experimental results of the two independent quantities ($\delta\nu \sim 260$ Hz and $I_{th} \sim 674$ mA) justifies the use of these latter parameter values.

A second interesting finding is obtained from the comparison between the measurements on RT and cryogenic QCLs: the intrinsic linewidth is larger at lower temperatures. A definitive test would be measuring the linewidth of QCL_1 at different heat-sink temperatures (for example 300 K and 80 K). Unfortunately, we have not been able to perform this experiment yet, because the QCL case does not fit our cryostat. Nevertheless, the theoretical model just used for predicting the values of the intrinsic linewidth can also be applied for predicting its dependence on temperature. In order to do this, we figure out the expected temperature-dependence of the intrinsic linewidth of QCL_1 in which, due to the temperature change, the pitch of the DFB grating is virtually tuned to match the lasing wavelength with peak-gain wavelength, thus keeping $\alpha_e \sim 0$. The ratio of the relaxation times at the two different temperatures is estimated to be $\tau_3(300\text{ K})/\tau_3(80\text{ K}) \simeq 0.6$ (a relatively small change even for such a large temperature change, because of the presence of alloy disorder scatterings). The coupling efficiency β is inversely proportional to the spectral width w_s of spontaneous emission, since this is the only

#152334 - $15.00 USD Received 3 Aug 2011; revised 18 Aug 2011; accepted 19 Aug 2011; published 29 Aug 2011

temperature-dependent term involved in β (see equation (A14) of Ref. [4]). From the experimental result of the spectral width of the present device we obtain the ratio of the coupling efficiencies $\beta(300\ \mathrm{K})/\beta(80\ \mathrm{K}) = w_s(80\ \mathrm{K})/w_s(300\ \mathrm{K}) \simeq 0.5$. On the other hand, the spontaneous emission lifetime τ_r and the photon decay rate γ are independent of temperature variations, as well as the small correction factor $\varepsilon \simeq 0.2$. Consequently, for $I_0/I_{th} \simeq 1.15$, the ratio of the intrinsic linewidths ($\propto \beta(\tau_3/\tau_r)\gamma$) is predicted to be $\delta\nu(300\ \mathrm{K})/\delta\nu(80\ \mathrm{K}) \simeq 0.3$. This can be considered a first theoretical confirmation of the dependence of the intrinsic linewidth on the operating temperature. Finally, we want to remark that the Schawlow-Townes-Henry formula [3] does not allow to evaluate the temperature dependence of the intrinsic linewidth.

Besides the comments on the intrinsic linewidth, the comparison between the low-frequency portion of QCL_1 and QCL_2 FNPSDs deserves further comments. The most relevant fact needing an explanation is the drastic reduction $(\delta f_2/\delta f_1)^2 \sim 200$ of the $1/f$–type frequency noise for the RT QCL (QCL_1). In Ref. [6], some experimental evidences were given to support the hypothesis that the flicker frequency noise originates from temperature fluctuations induced by an internal tunnelling-current flicker noise δI: $\delta f \propto \delta T \sim R_{therm}\delta P \propto R_{therm}\delta I$. As a consequence, the frequency noise reduction is given by:

$$\left(\frac{\delta f_2}{\delta f_1}\right)^2 \propto \left(\frac{R_{therm2}}{R_{therm1}}\right)^2 \times \left(\frac{\delta I_2}{\delta I_1}\right)^2 \tag{3}$$

Hence, a comparison between the thermal resistances and the flicker current noise of the RT and the cryogenic devices could help in identifying the origin of the large difference between the $1/f$-type frequency noise of QCL_1 and QCL_2. This is further validated by the fact that all other key parameters involved in the comparison, such as injection barrier thickness, number of periods, thickness of one period and interface density are only sligthly different between the two devices (respectively 3.5 nm, 25, 51.7 nm and 425.53 $\mu\mathrm{m}^{-1}$ for QCL_1 [9] and 4.6 nm, 22, 57.7 nm and $\sim 390\ \mu\mathrm{m}^{-1}$ for double-phonon design [16] QCL_2 with a $\sim 11\ \mu$m bare ridge waveguide, a shorter cavity length of 1.5 mm, a comparable injector doping density of $\sim\ 3\times\ 10^{11}\ \mathrm{cm}^{-2}$ and epi-side-up mounting; see Refs. [17, 18] for the definition of the interface density). On the contrary, by considering the temperature-dependent cross-plane thermal resistivity [19], and scaling for the different device length, the mounting geometry (epi-side up or down) and the active region temperature, the thermal resistance R_{therm2} of QCL_2 is convincingly inferred to be about 6 times higher than that of QCL_1: $R_{therm2} \sim 6R_{therm1} \sim 44.5$ K/W. This higher thermal resistance well explains the observed thermal cut-off at 200 kHz for QCL_2, as shown in Fig. 2(a) and also in Ref. [6], though the thermal cut-off for QCL_1, expected at around 1 MHz, is unfortunately masked by spurious noise. However the scaling of thermal resistance can only partially explain the huge reduction of the flicker FNPSD of Eq. 3 (a factor 36 vs. 200). An additional effect involving the internal current squared fluctuations δI^2 must be assumed for explaining the remaining factor $200/36 \simeq 5.5$. Switching from current to current-density squared fluctuations δJ^2 leads to an expected reduction of $(\delta J_2/\delta J_1)^2 \simeq 22$, since the active region dimensions only differ for a factor two in length. This behavior could eventually involve the alternate capture and emission of electrons at individual quantum sites (defect sites in case of homogeneous semiconductors) which is known to generate discrete switching in the device resistance and, consequently, current fluctuations. A single occurrence of this effect is referred to as a random telegraph signal (RTS), and the summation of many RTSs in structured devices like QCLs may result in $1/f$ noise. The emission and trapping rates are expected to be proportional to the exponential form $\exp(-E_a/k_BT)$, which means that the rate drastically increases with temperature. Here, the experimental results suggest the following hypothesis: at higher rates the contributions of individual RTSs may cancel out more effectively, resulting in a lower 1/f noise. Basing on these considerations we assume, for the squared current-density flicker

#152334 - $15.00 USD Received 3 Aug 2011; revised 18 Aug 2011; accepted 19 Aug 2011; published 29 Aug 2011

noise, an inverse exponential form $\delta J^2 \propto 1/\exp(-2E_a/k_BT)$. Consequently, the factor 22 in the ratio of squared current-density fluctuations $(\delta J_2/\delta J_1)^2 = \exp(2E_a/k_BT_2)/\exp(2E_a/k_BT_1)$ leads to an empirical estimation of the activation energy $E_a \sim$ 50 meV, which is comparable to thermal energies in the considered temperature range. A deeper investigation is required in order to give a more reliable and quantitative treatment. Nevertheless, the discussion presented above adds valuable elements supporting the correlation between internal current fluctuations and flicker fluctuations in the electron populations of the QCL quantum structure.

Finally, we want to discuss some perspectives concerning linewidth reduction of our RT QCL, based on the experimental data shown above. First, we must conclude that a further improvement of the laser driver current noise is required in order to fully exploit the drastic reduction of the QCL frequency noise. The noise level, currently in the range of 1–2 nA/$\sqrt{\text{Hz}}$, needs to be lowered down of at least one order of magnitude. Alternatively, a low-pass filtering on the current output should be implemented, at the expense of the modulation bandwidth of the driver. In this frame, it is possible to implement a frequency-locking loop acting on the driving current for a reduction of the laser linewidth. Following Ref. [5], from the experimental FNPSD of the RT QCL we calculate a free-running linewidth of about 400 kHz (FWHM) over an observation time of 10 ms. This is not a suitable linewidth for demanding spectroscopic experiments in the mid-infrared range. As an example, the present broad free-running linewidth of our QCL limits its application to the case of ultra-high-sensitivity Saturated-Absorption Cavity-Ring-down spectroscopy (see Ref. [20]), since it requires laser radiation coupling to a high-finesse cavity mode with a few kHz width. Indeed, mid-IR QCLs can be combined with well-established techniques [21] to efficiently narrow their linewidth even below the intrinsic levels, as demonstrated in a pioneering work by Taubman et al. [22]. Following the recent work by Di Domenico et al. [23], we can conclude that with moderate bandwidth (less than 100 kHz) and gain (about 50 dB at 10 Hz) a narrowing of the QCL source down to the kHz level can be easily achieved. Comparable narrowing of the cryogenic QCL would clearly require a larger servo loop bandwidth, given its measured FNPSD.

5. Conclusions

In this work the frequency-noise power spectral density of a room-temperature QCL at 4.3 μm is completely characterized. An intrinsic linewidth of 260 Hz, about four times smaller than in a cryogenic QCL, is measured, in reasonable agreement with the theoretical value. The flicker $1/f$–type frequency noise, occurring at lower frequencies, is also drastically reduced (about a factor 200) with respect to the case of a cryogenically-operated QCL at the same wavelength. A physical interpretation of the measured behaviour is proposed, based on the hypothesis that the flicker frequency noise originates from temperature fluctuations induced by an internal tunnelling-current flicker noise. The temperature dependence of both the thermal resistance and the current flicker noise well explains the experimental results, assigning a predominant effect of the heterostructure in determining the shape and amplitude of the FNPSD curve. In conclusion, if an important element for the success of QCLs has undoubtedly been the tailoring of their emitted frequency, we believe that tailoring of QCLs spectral features is now possible and it can be the key for their next most demanding applications.

Acknowledgments

We gratefully acknowledge Dr. Pablo Cancio Pastor for his critical reading of the manuscript and M. Giuntini, A. Montori and M. De Pas from LENS for their help on driving electronics. This work was partially supported by Ente Cassa di Risparmio di Firenze and by Regione Toscana through the projects CTOTUS and SIMPAS, in the framework of POR–CReO FESR 2007–2013.

#152334 - $15.00 USD Received 3 Aug 2011; revised 18 Aug 2011; accepted 19 Aug 2011; published 29 Aug 2011